Article

Cell Reports

FBH1 Catalyzes Regression of Stalled Replication Forks

Graphical Abstract

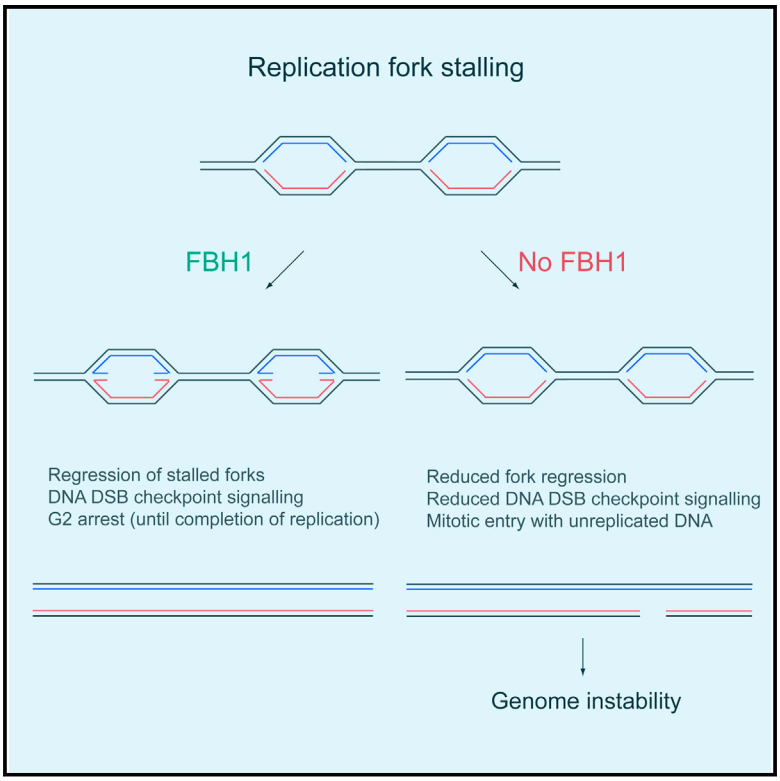

Authors

Kasper Fugger, Martin Mistrik, ...,
Ian D. Hickson, Claus Storgaard Sørensen

Correspondence

css@bric.ku.dk

In Brief

It is unclear how stalling DNA replication forks are being processed in order to preserve genome stability. Here, Fugger et al. demonstrate that FBH1, through its helicase activity, catalyzes the reversal of stalling DNA replication forks in vivo and in vitro and promotes checkpoint signaling to promote genome integrity.

Highlights

- FBH1 helicase plays a major role in remodeling of stalled DNA replication forks
- FBH1 is required for DNA replication fork reversal in vivo
- FBH1 helicase directly catalyzes fork reversal in vitro
- ATM checkpoint signaling following replication fork stalling depends on FBH1

Fugger et al., 2015, Cell Reports *10*, 1749–1757
March 17, 2015
http://dx.doi.org/10.1016/j.celrep.2015.02.028

CellPress

Cell Reports
Article

FBH1 Catalyzes Regression of Stalled Replication Forks

Kasper Fugger,[1] Martin Mistrik,[2] Kai J. Neelsen,[3,6] Qi Yao,[4] Ralph Zellweger,[3] Arne Nedergaard Kousholt,[1] Peter Haahr,[1] Wai Kit Chu,[4,6] Jiri Bartek,[2,5] Massimo Lopes,[3] Ian D. Hickson,[4] and Claus Storgaard Sørensen[1,*]
[1]Biotech Research and Innovation Centre (BRIC), University of Copenhagen, Ole Maaløes Vej 5, 2200 Copenhagen N, Denmark
[2]Institute of Molecular and Translational Medicine, Faculty of Medicine and Dentistry, Palacky University Olomouc, Hnevotinska 5, 77900 Olomouc, Czech Republic
[3]Institute of Molecular Cancer Research, University of Zürich, Winterthurerstrasse 190, 8057 Zürich, Switzerland
[4]Center for Healthy Aging, Department of Cellular and Molecular Medicine, University of Copenhagen, Panum Institute, Blegdamsvej 3B, 2200 Copenhagen N, Denmark
[5]Danish Cancer Society Research Centre, Strandboulevarden 49, 2100 Copenhagen O, Denmark
[6]Present address: The Novo Nordisk Foundation Center for Protein Research, Blegdamsvej 3B, 2200 Copenhagen, Denmark
*Correspondence: css@bric.ku.dk
http://dx.doi.org/10.1016/j.celrep.2015.02.028

SUMMARY

DNA replication fork perturbation is a major challenge to the maintenance of genome integrity. It has been suggested that processing of stalled forks might involve fork regression, in which the fork reverses and the two nascent DNA strands anneal. Here, we show that FBH1 catalyzes regression of a model replication fork in vitro and promotes fork regression in vivo in response to replication perturbation. Cells respond to fork stalling by activating checkpoint responses requiring signaling through stress-activated protein kinases. Importantly, we show that FBH1, through its helicase activity, is required for early phosphorylation of ATM substrates such as CHK2 and CtIP as well as hyperphosphorylation of RPA. These phosphorylations occur prior to apparent DNA double-strand break formation. Furthermore, FBH1-dependent signaling promotes checkpoint control and preserves genome integrity. We propose a model whereby FBH1 promotes early checkpoint signaling by remodeling of stalled DNA replication forks.

INTRODUCTION

Perturbation of DNA synthesis often leads to stalling of the DNA replication fork. In the case of widespread fork stalling, cells enter a state commonly referred to as "replication stress" (Branzei and Foiani, 2010; Ciccia and Elledge, 2010; Jackson and Bartek, 2009). Several drugs have been used to study the replication stress response, including hydroxyurea, which causes stalling of replication forks due to depletion of dNTPs. Several factors are known to recognize and act on stalled forks, and this leads ultimately to activation of checkpoint responses, as well as repair and restart of the fork. These responses are mediated through enzymatic remodeling of the stalled forks; however, the mechanisms are in many circumstances not understood. An emerging regulator of the response to stalled replication forks is the FBH1 helicase. FBH1 is a member of the conserved UvrD family of 3′-5′ DNA helicases that has been shown to operate on a number of cellular substrates including stalled replication forks (Kim et al., 2002; Masuda-Ozawa et al., 2013). FBH1 was shown recently also to efficiently promote MUS81-induced DNA breakage and p53 activation following long-term HU treatment that leads to fork collapse (Fugger et al., 2013; Jeong et al., 2013b). In line with a role of FBH1 in replication stress responses, FBH1 was shown to accumulate at the stalled fork shortly after exposure to HU (Fugger et al., 2009). However, the functional role of FBH1 recruitment to stalled forks and whether and how FBH1 may contribute to the early stage processing of stalled forks is still unclear. To gain insights into these fundamental issues, we undertook to investigate the role of FBH1 in response to short-term replication stress.

RESULTS

FBH1 Catalyzes Fork Regression In Vitro

It has been shown previously that FBH1 is recruited to ssDNA areas following HU-induced fork stalling (Fugger et al., 2009) and that FBH1 can unwind the lagging strand (Masuda-Ozawa et al., 2013). Therefore, we hypothesized that FBH1 might be involved in remodeling of stalled forks due to its helicase activity. Regressed forks result from backtracking of the fork and the pairing of the nascent leading and lagging strands (Atkinson and McGlynn, 2009). To address a putative role of FBH1 in this process, we tested whether purified recombinant FBH1 (Simandlova et al., 2013) could catalyze fork regression using a previously validated substrate resembling a replication fork (Ralf et al., 2006; Figure 1A). We found that FBH1 possesses a concentration-dependent fork-regression activity (Figure 1B), indicating that FBH1 can promote fork regression in vitro. To further substantiate this finding, we repeated the assay with helicase-deficient FBH1, which did not promote regression of the model fork substrate (Figure 1C). Consistent with this, FBH1-mediated

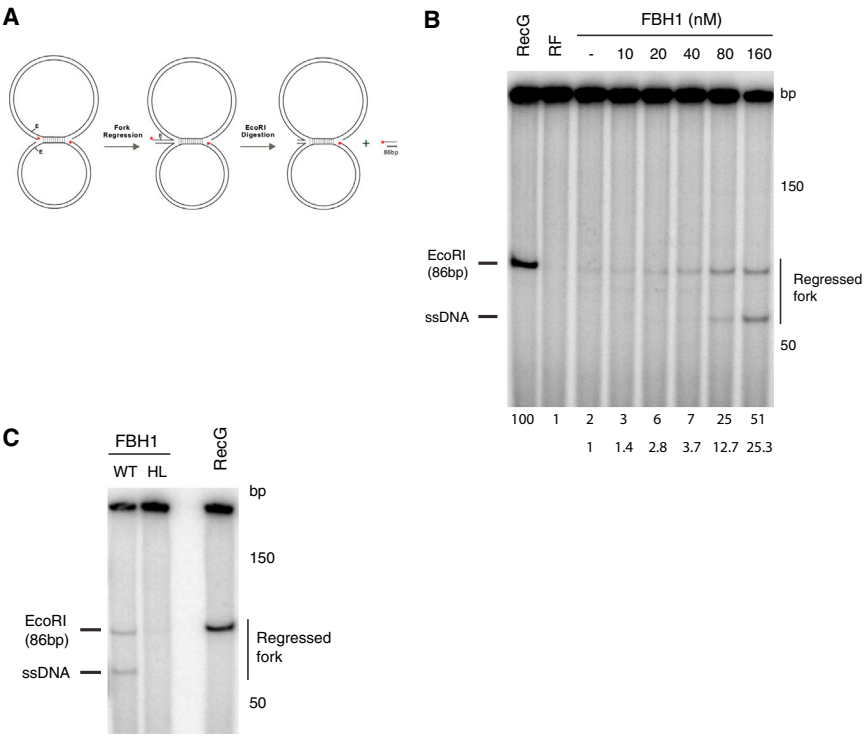

Figure 1. FBH1 Catalyzes Fork Regression In Vitro

(A) Schematic representation of the substrate used in the fork-regression assay.

(B) Indicated concentration of FBH1 was incubated with 5 pM replication fork substrate at 37°C for 30 min and then digested with EcoRI. The reaction products were separated by native PAGE. Gels were dried and processed by PhosphorImaging. RecG, a bona fide bacterial fork regressor, was included as a positive control.

(C) FBH1 wild-type (WT) or helicase dead (HL) were incubated with 5 pM replication fork substrate at 37°C for 30 min and then digested with EcoRI. The reaction products were separated by native PAGE. Gels were dried and processed by PhosphorImaging.

regression was dependent on ATP hydrolysis, indicating that FBH1 catalyzes fork regression through its helicase domain in an ATP-dependent manner (Figure S1A). To compare the activity of FBH1 to another bona fide fork regressor, BLM (Ralf et al., 2006), we carried out comparative fork-regression assays. We found that the two helicases were able to generate similar products; however, the activity of FBH1 was slightly higher than that of BLM (Figure S1B). Taken together, these data indicate that FBH1 is a fork-regressing helicase in vitro. The ssDNA product generated by FBH1 and BLM helicases (Figure S1B), in addition to the dsDNA regression product, is commonly observed due to partial unwinding of the dsDNA product. This is not seen with RecG, which lacks significant DNA helicase activity.

FBH1 Is Required for Fork Regression In Vivo

These initial findings prompted us to investigate whether FBH1 might be involved in fork regression in vivo. To do this, we first analyzed whether replication forks stalled by treatment with HU might be prone to regress. Using electron microscopy (EM) (Neelsen et al., 2014) to visualize replication intermediates (Figure 2A), we found an approximately 4-fold increase in the occurrence of regressed forks in HU-treated cells compared to mock-treated cells (Figure 2B). Genomic DNA was crosslinked prior to lysis to preserve intracellular fork structures during DNA isolation and spreading. Importantly, we found that depletion of FBH1 resulted in a 2-fold decrease in HU-induced fork regression (Figure 2B), suggesting that FBH1 promotes at least a proportion of the observed regression of stalled replication forks in vivo. In contrast to its role in fork regression, we did not find evidence that FBH1 affects resection of the regressed forks as measured by the presence of ssDNA at the regressed arm (Figure S1C). Hence, our data define FBH1 as the first enzyme that promotes fork regression in vivo in higher eukaryotes. To substantiate the data from EM studies, we utilized a recently reported indirect approach for detecting intermediates with unwound newly synthesized strands, including regressed forks (Couch et al., 2013). This involves the use of the nucleotide analog, BrdU, the epitope for which is masked under normal circumstances and is only detectable when exposed on ssDNA (Figure S1D). Using this method, we found that HU treatment resulted in a significant increase in ssDNA exposure of the nascent DNA strands as evidenced by BrdU foci, indicative of fork remodeling and possibly regression (Figures 2C and 2D). In support of the EM data, we found that this nascent strand exposure was dependent upon FBH1 (Figures 2C and 2D), further implying that efficient HU-induced fork regression depends on FBH1.

To further strengthen the notion that FBH1 can actively promote fork regression in vivo, in a helicase-dependent manner, we carried out the native BrdU assay in cells after inducing expression of either wild-type (WT) or helicase-dead FBH1. We found that the HU-induced fork processing as measured by ssDNA exposure was augmented in the presence of FBH1 WT, but not a helicase-dead allele (Figures 2E and 2F). In addition to this, we found that overexpression of helicase-dead FBH1 suppressed ssDNA formation compared to the non-induced HU-treated control, which argues that the helicase-deficient allele inhibits endogenous FBH1 in a dominant-negative fashion through its homo-dimeric interaction (Fugger et al., 2013).

Collectively, our data suggest that FBH1 directly promotes regression of stalled replication forks in vivo through its helicase activity.

FBH1 Promotes DSB Checkpoint Signaling from Stalled Forks

We and others have shown previously that FBH1 is required for fork cleavage and checkpoint signaling following prolonged fork stalling, which is linked to DNA breakage (Fugger et al., 2013; Jeong et al., 2013b). We reasoned that the fork-regression

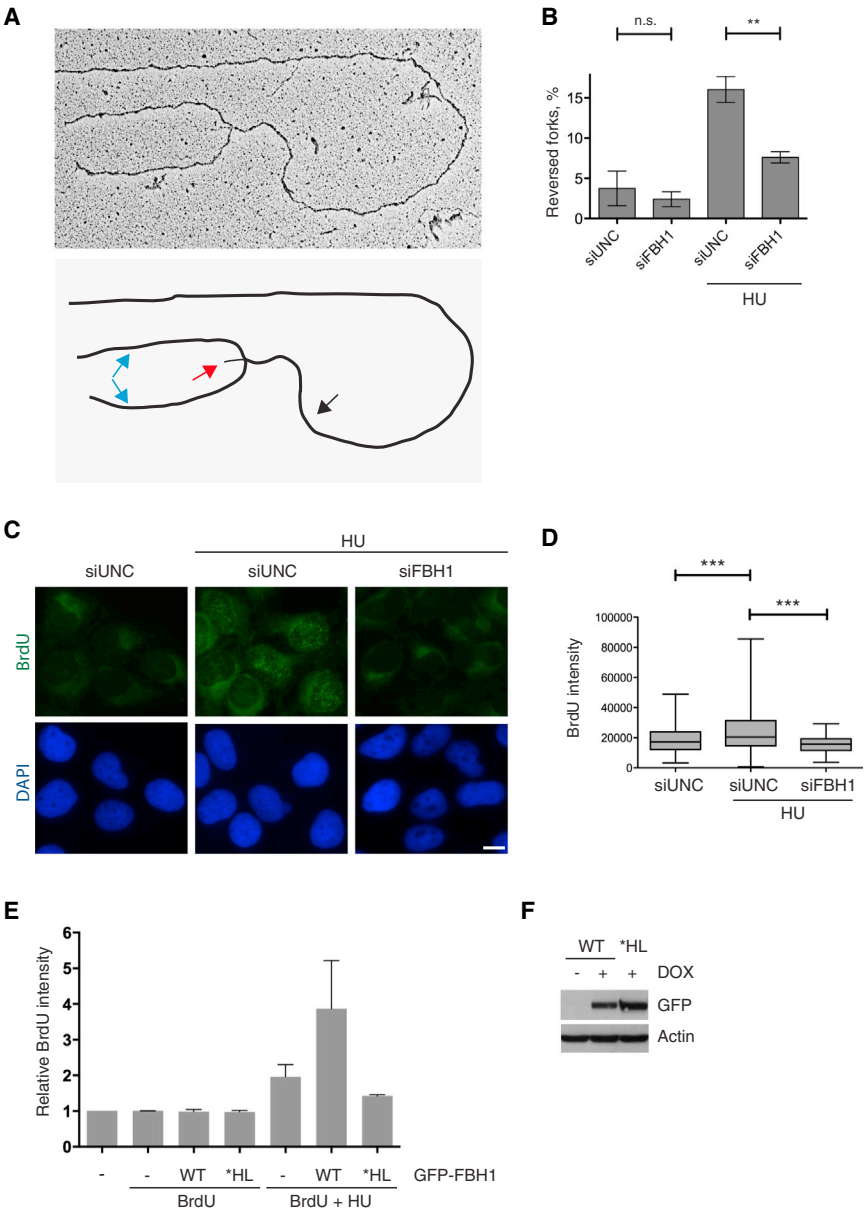

Figure 2. FBH1 Mediates Fork Regression In Vivo

(A) (Top) U2OS cells were transfected with control or FBH1 siRNA for 48 hr before treatment with 2 mM HU for 4 hr before psoralene crosslinking. Genomic DNA was extracted and prepared for EM, and images were acquired using TEM. (Bottom) Graphical representation of a regressed replication fork; nascent strands (blue arrow), parental strand (black arrow), regressed arm (red arrow).

(B) Quantification and statistical analysis of regressed forks from (A) was performed using Graphpad Prism 6 software. At least 70 replication intermediates were analyzed for each condition. Error bars represent SD from three independent experiments.

(C) U2OS cells were seeded on coverslips and transfected with control or FBH1 siRNA for 48 hr. Cells were then pulse labeled with 10 μM BrdU for 10 min and subsequently treated with HU for 4 hr before fixation. Cells were subjected to immunofluorescence with anti-BrdU antibody, and images were acquired using AxioVert microscope. Image analysis was performed using Volocity software. The scale bar represents 10 μm.

(D) Quantification and statistical analysis of BrdU intensity of samples from (C) were performed using Graphpad Prism 6 software. Boxplot with whiskers representing min to max values.

(E) U2OS cells expressing either WT or helicase mutant (*HL) GFP-FBH1 in a doxycycline-inducible fashion were seeded on coverslips, and expression was induced or not for 24 hr. Cells were then pulse labeled with 10 μM BrdU for 10 min and subsequently treated or not with HU for 4 hr before fixation. Cells were subjected to immunofluorescence with PCNA and anti-BrdU antibody, and images were acquired using the Olympus ScanR system (as described in the Experimental Procedures section). Quantification and statistical analysis was performed using Graphpad Prism 6 software. Error bars represent SD.

(F) Immunoblotting of samples from (E) showing GFP-FBH1 expression.

activity of FBH1 might also be involved in early signaling elicited from stalled forks. To address the role of FBH1 following short-term HU treatment, which causes stalling, but not collapse, of the fork, we used a cell line carrying an FBH1-specific shRNA expressed under the control of a doxycycline-inducible promoter. Cells depleted for FBH1 displayed a marked reduction in phosphorylation of RPA on Ser4 and Ser8 following HU treatment for 0.5–4 hr, both in the chromatin-bound fraction and in the total cellular pool (Figure 3A). The enzymology underlying RPA hyperphosphorylation is not fully understood, but it has been associated with checkpoint signaling following DNA breakage, such as via DNA-PK activity (Bunting et al., 2010; Liaw et al., 2011). Moreover, the ATM-mediated phosphorylation of CHK2 on Thr68, and the phosphorylation-induced electrophoresis mobility shift of the DNA end resection factor, CtIP, were both markedly reduced following HU treatment of FBH1-depleted cells (Figure 3A). This is in agreement with previous data showing that depletion of FBH1 leads to a reduction of ATM-mediated signaling after 8 hr treatment of HU (Jeong et al., 2013b). Unexpectedly, however, considering the known role of the ATR-CHK1 pathway in response to replication stress, we found that ATR-CHK1 signaling was unaffected by depletion of FBH1 (Figure 3A).

In addition to HU, a number of other agents and drugs interfere with the replication fork, leading to fork stalling. To test whether FBH1 was also required for checkpoint signaling in response to other types of fork stalling, we treated cells with thymidine and low-dose camptothecin, which does not lead to readily detectable DNA DSB formation at this concentration (Figure S2A). Although we found that checkpoint signaling following HU treatment was most sensitive to FBH1 depletion, signaling following

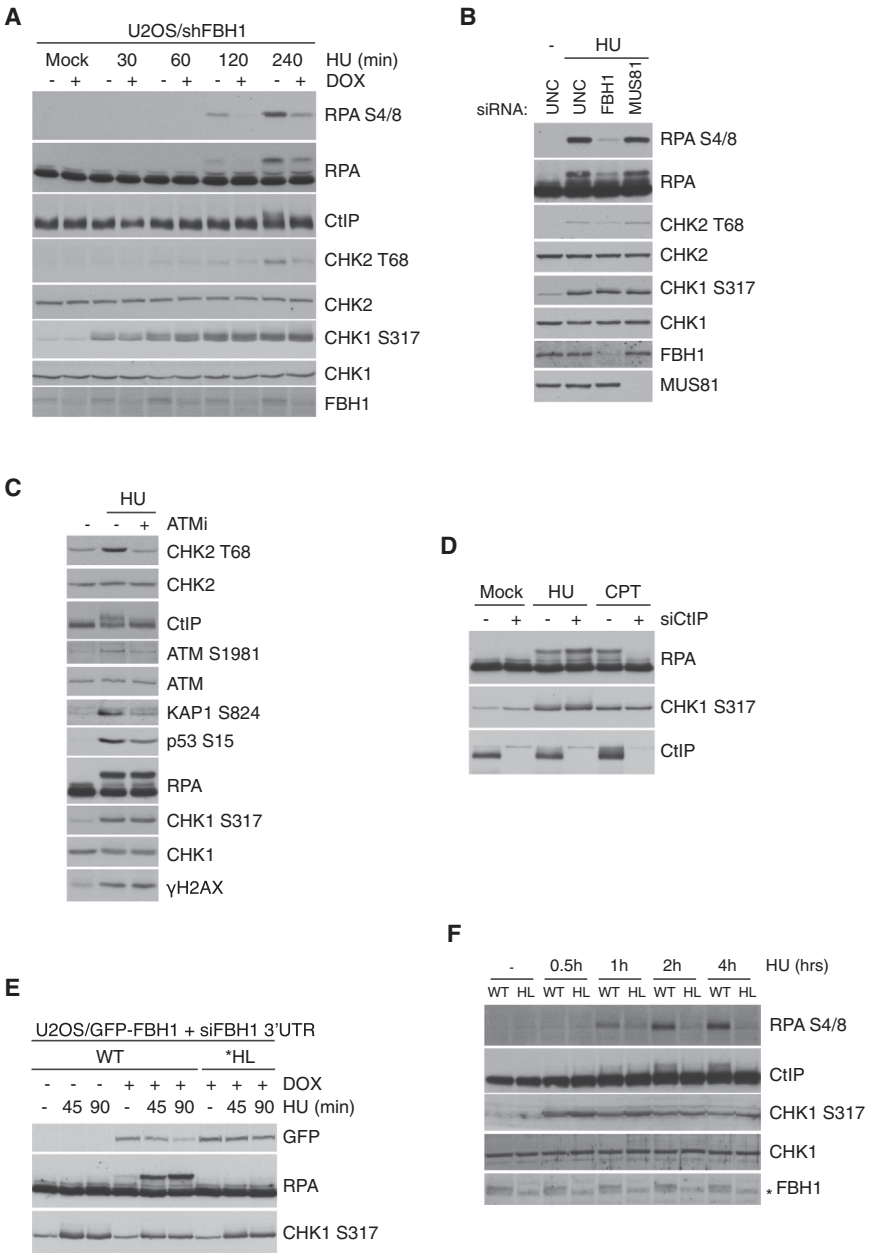

Figure 3. FBH1 Mediates DNA DSB Checkpoint Signaling through Its Helicase Activity following Replication Fork Stalling

(A) U2OS/shFBH1 cells were either induced or not with doxycycline for 48 hr before treatment with 2 mM HU. Cells were collected at the indicated time points and subjected to immunoblotting with the indicated antibodies.

(B) U2OS cells were transfected with FBH1 or MUS81 siRNA for 48 hr. Cells were treated with 2 mM HU for 4 hr, collected, and subjected to immunoblotting with the indicated antibodies.

(C) U2OS cells were either untreated or pre-treated with an ATM inhibitor (10 μM) for 30 min prior to treatment with either 2 mM HU for 4 hr or 1 μM CPT for 1 hr. Cells were collected and subjected to immunoblotting with the indicated antibodies.

(D) U2OS cells were transfected with UNC or CtIP siRNA for 48 hr. Cells were either left untreated or treated with 2 mM HU for 4 hr, collected, and subjected to immunoblotting with the indicated antibodies.

(E) U2OS cells expressing either human WT or *HL GFP-FBH1 in a doxycycline-inducible fashion were depleted using siFBH1 targeting in the 3′ UTR for 48 hr. Expression of GFP-FBH1 was induced 24 hr post-transfection. Cells were either left untreated or treated with 2 mM HU for the indicated times, collected, and subjected to immunoblotting.

(F) MESCs, either FBH1 WT or HL were treated with 0.5 mM HU, collected at the indicated time points, and subjected to immunoblotting with the indicated antibodies. Asterisk indicates a cross-reacting band.

treatment with thymidine or low-dose CPT was also partially dependent on FBH1 (Figure S2A). This suggests that FBH1 operates in response to several types of replication stress, where it may modulate the structure of the fork in order to elicit efficient checkpoint signaling through key replication and repair factors such as RPA and CtIP.

DSB Checkpoint Signaling Occurs in the Absence of Detectable DNA Breaks

The phosphorylation of RPA and CtIP has been reported to occur after DSB formation (Bunting et al., 2010; Li et al., 2000). In a time course experiment combining western blotting and pulsed-field gel electrophoresis (PFGE), we found, however, that these phosphorylation events occurred in a time frame (2–12 hr) where DSBs were not readily detectable. Indeed, detectable HU-induced DNA breaks did not appear until 24 hr after HU addition, in agreement with previous findings (Figure S2B, bottom; Hanada et al., 2007; Petermann et al., 2010). To rule out the possibility that breaks were not detected at early time points due to the limitations of the PFGE assay, we treated cells with the topoisomerase I inhibitor CPT that, at the high dose used, induces DSBs at replication forks (Ryan et al., 1991). Already 30–60 min after addition of CPT, we could observe a moderate accumulation of DNA breaks (Figure S2C), despite the fact that the intensity of DSB signaling through RPA and CtIP was comparable to that after only 4 hr of HU treatment (Figure S2D). Therefore, the strong HU-induced ATM-mediated signaling probably originates either from a very small number of DSBs or from the generation of other types of DNA structures at the stalled replication forks.

We investigated further the potential role of DNA DSB formation because prolonged HU treatment leads to the collapse of stalled replication forks accompanied by DNA breakage mediated by FBH1 and the MUS81 endonuclease (Fugger et al.,

2013; Hanada et al., 2007; Jeong et al., 2013b). Ablation of MUS81, therefore, prevents the accumulation of DSBs following HU treatment. To test whether prevention of MUS81-specific DNA breakage would have any impact on the observed checkpoint signaling, we depleted MUS81 using siRNA. Depletion of MUS81 did not have any effect on ATM-mediated phosphorylation of either CHK2 or RPA at early times after HU treatment, further supporting the notion that FBH1 promotes checkpoint signaling through events that precede and are independent of marked DNA DSB formation (Figure 3B).

DSB Signaling Occurs in an ATM-Dependent but Resection- and Recombination-Independent Manner following Fork Stalling

HU treatment is known to activate ATR through the formation of RPA-coated ssDNA (Cimprich and Cortez, 2008), which raised the possibility that the apparent ATM-dependent checkpoint signaling to CtIP was instead mediated by ATR. Using an ATM-specific inhibitor (Hickson et al., 2004), we found a clear reduction in the HU-mediated phosphorylation of CtIP, ATM, CHK2, KAP1, and p53, but not of CHK1, γH2AX, or RPA (Figure 3C), suggesting that HU does indeed induce ATM activation within a time frame where DNA DSBs are not detectable. Hyperphosphorylation of RPA has been shown to occur following DNA breaks in a CtIP-dependent fashion through resection of the DNA ends (Sartori et al., 2007). Given that CtIP was highly phosphorylated and presumably activated in response to HU treatment, we tested whether the RPA phosphorylation was dependent on the activity of CtIP. However, in contrast to high-dose CPT treatment, we did not find any dependency on CtIP for RPA phosphorylation following HU treatment, suggesting that this modification occurs by a resection-independent mechanism (Figure 3D). Interestingly, it was recently shown that hyperphosphorylation of RPA is important for preserving genome integrity during replication stress (Ashley et al., 2014). Taken together, our data define a critical role for FBH1 upstream of the RPA hyperphosphorylation at early stages in response to replication fork stalling, where it might serve to protect and/or rescue replication forks that have stalled through efficient checkpoint signaling.

Next, we investigated how FBH1 could affect the response to fork stalling. FBH1-ablated cells have been shown to form spontaneous RAD51 foci (Fugger et al., 2009; Laulier et al., 2010; Lorenz et al., 2009). To test the possibility that increased chromatin-bound RAD51 could protect replication forks from being processed and thus lead to reduced DNA DSB signaling, cells were depleted of RAD51 and treated with HU. However, we found no evidence for a rescue of the decreased HU-induced signaling in FBH1-depleted cells by co-depletion of RAD51, but rather a further decrease in checkpoint response was seen, most likely due to the cell-cycle delay observed in RAD51-depleted cells (Figure S2E; data not shown). This suggests that the specific effect of FBH1 depletion on these signaling events occurring after HU treatment is independent of RAD51.

FBH1 Promotes DSB Signaling through Its Helicase Activity

The lack of detectable DNA breakage following short-term HU treatment combined with the strong DSB-like signaling suggested to us that FBH1 mediates rearrangement of stalled forks into structures that provides the basis for the observed signaling. Given our data indicating that FBH1 catalyzes fork regression, it seemed plausible that the checkpoint signaling might in principle involve the regressed fork because this would form a free DNA end that resembles a conventional DNA DSB with a resected end, which is known to be capable of inducing checkpoint signaling (Ray Chaudhuri et al., 2012). To test this hypothesis, we assessed the contribution of the helicase activity of FBH1 to the checkpoint signaling seen following replication arrest. Using siRNA targeting the 3′ UTR of FBH1, we could reconstitute cells with ectopic expression of FBH1 using the doxycycline-inducible system described above. Whereas cells depleted for FBH1 did not show any detectable phospho-RPA 90 min after HU treatment, induction of wild-type FBH1, but not a helicase-dead version, could completely rescue RPA phosphorylation in response to HU treatment (Figure 3E). This indicates that FBH1 promotes checkpoint signaling through a helicase-dependent mechanism at early time points after fork stalling.

To substantiate our findings, we used mouse embryonic stem cells (MESCs) carrying biallelic deletions in the FBH1 helicase domain (Fugger et al., 2013). Upon treatment with HU, the WT MESCs showed a time-dependent increase in RPA and CtIP phosphorylation that paralleled that of human cells, albeit with slightly faster kinetics (Figure 3F). However, the FBH1 helicase-deficient cells (HL) displayed almost complete abrogation of RPA and CtIP phosphorylation following HU treatment, in agreement with the findings in human cells.

FBH1 Is Required for G2 Checkpoint Control and Genome Maintenance following Fork Stalling

ATM is a key factor in checkpoint pathways (Thompson, 2012), and our finding that FBH1 promotes ATM activation following fork stalling prompted us to investigate whether FBH1 plays a role in cell-cycle control. To this end, we released cells from a HU block and followed their progression through S phase and into mitosis. We did not observe any obvious difference in S phase progression between control and FBH1-depleted cells (Figure S3A). Interestingly, however, we found that the FBH1-depleted cells released from an arrest induced by HU entered mitosis faster than did control cells (Figure 4A). In line with this, we found that FBH1-depleted cells released from the HU-induced arrest had a much-faster decay of the DSB-related checkpoint response, as seen by a rapid decrease in RPA phosphorylation (Figures S3B and S3C). Taken together, this indicates that cells released from an HU block traverse S phase with an active checkpoint but then become delayed in the G2 phase via the FBH1-mediated G2/M checkpoint. This G2 delay could provide time to complete DNA repair and finish replication in areas of the genome with persistently inactivated forks. Because FBH1-deficient cells exhibit an aberrant checkpoint control following replication stress, we asked whether these cells released from HU arrest would show signs of incomplete replication in the ensuing G1 phase. To this end, we chose to investigate the formation of 53BP1 bodies in G1 cells, which has been associated with fragile sites and difficult-to-replicate regions of the genome (Harrigan et al., 2011; Lukas et al., 2011). Whereas depletion of FBH1 itself did not lead to an increase in 53BP1

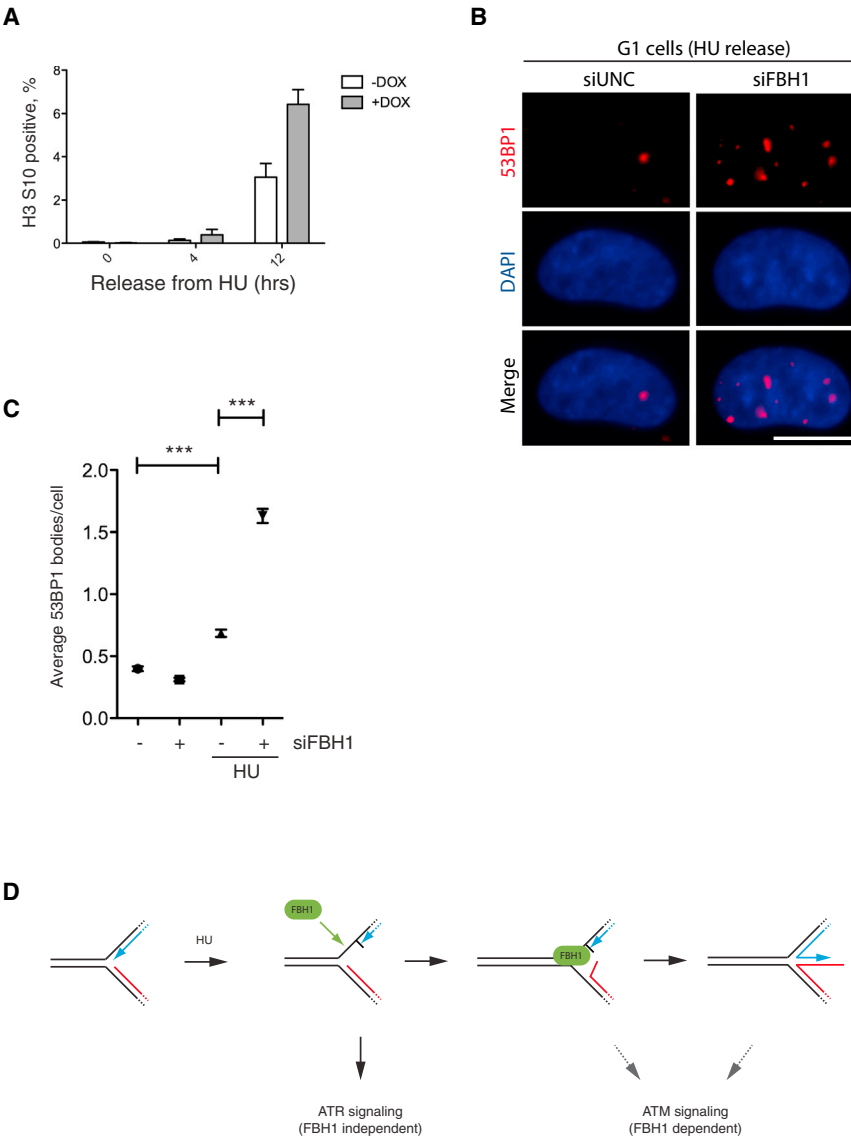

Figure 4. FBH1 Promotes Checkpoint Control and Genome Integrity

(A) U2OS/shFBH1 were either induced or not with doxycycline for 48 hr before treatment with 2 mM HU for 16 hr. Cells were released from the HU block into fresh media containing nocodazole (100 ng/ml) and collected at the indicated time points, stained with phospho-H3-S10 antibody, and analyzed by flow cytometry. Statistical analysis was performed using Graphpad Prism 6 software. Error bars represent SD.

(B) TIG3 cells were seeded on coverslips and transfected with UNC or FBH1 siRNA for 48 hr before treatment with HU for 18 hr. Cells were released for 24 hr, fixed, and subjected to immunofluorescence as described in the Experimental Procedures section. Single-cell images of 53BP1 foci were acquired using the ScanR system (see Experimental Procedures). The scale bar represents 10 μm.

(C) Quantification of 53BP1 foci from at least 5,000 G1 cells. Statistical analysis was performed using Graphpad Prism 6 software. Error bars represent mean with 95% CI.

(D) Model depicting how FBH1 mediates fork processing and promotes checkpoint signaling (see text for details).

body formation, treatment with HU led to a slight increase in the frequency of 53BP1 bodies, which was significantly augmented in cells depleted for FBH1 (Figures 4B and 4C). These data argue that the FBH1-mediated checkpoint control following replication stress is important to ensure a proper control of cell-cycle progression to guard genome integrity.

DISCUSSION

The mechanisms by which stalled forks are processed are not well understood in mammalian cells. We have identified FBH1 as the first enzyme responsible for fork regression in vivo in higher eukaryotes. The fact that FBH1 possesses fork-regression activity in vitro supports our notion that FBH1 is a bona fide fork-regression enzyme in mammalian cells. FBH1 has also been shown to specifically unwind the lagging strand of stalled forks in vitro (Masuda-Ozawa et al., 2013), suggesting that FBH1 could theoretically cooperate with 5′-3′ helicases in vivo to augment the regression process.

Replication arrest does not induce detectable DNA DSB formation at early times after HU treatment. In spite of this, we observed that HU induces a marked FBH1-dependent DNA-DSB-like signaling response soon after HU treatment, as evidenced by the phosphorylation of DSB-related ATM targets. Moreover, upon depletion of MUS81, which is required for DNA breakage following prolonged exposure to HU, we observed no effect on checkpoint signaling. This suggests that the DSB signaling is induced by either a very small number of DNA DSBs or even in the absence of breaks. Our data imply a conceptually new signaling pathway, whereby stalled forks are processed by FBH1 to form DNA structures with ability to signal like DNA DSB structures. This could, in principle, be explained by an accumulation of regressed replication forks following HU treatment, a structure that, through pairing of the nascent strands, generates a free DNA end (Figure 4D).

In addition to the situation of HU-induced fork stalling described here, regressed forks have also been observed upon topoisomerase inhibition by low-dose CPT (Ray Chaudhuri et al., 2012), after cyclin-E- and CDC25A-induced deregulation of the replication program (Neelsen et al., 2013a) and in the presence of template discontinuities (Neelsen et al., 2013b). FBH1 has strong affinity for ssDNA (Fugger et al., 2009) and markedly accumulates at HU-stalled forks. This may be one of the defining structural features that underlie the ability of FBH1 to promote

fork reversal after short-term HU. Interestingly, fork reversal in the absence of detectable DSB correlated with DNA DSB signaling after low-dose CPT treatment (Ray Chaudhuri et al., 2012) but did not elicit a similar response under cyclin-E-induced deregulation of the replication program (Neelsen et al., 2013a), suggesting that fork reversal per se is insufficient to activate the checkpoint. It is possible that DSB-independent ATM signaling upon fork stalling is dependent on specific molecular features of the induced reversed forks, which may escape detailed identification by EM analysis. Furthermore, ATM signaling from double-stranded ends at regressed arms may also require binding of cellular mediators or removal of replicative factors, which may only occur upon specific conditions of replication stress.

Collectively, our data link a novel FBH1 fork-remodeling activity with checkpoint signaling that operates after the ATR-CHK1 pathway is activated (Figure 4D). Notably, this FBH1-mediated checkpoint response to fork stalling is active prior to the MUS81-catalyzed accumulation of DNA DSBs. Recently, phosphorylation of RPA on Ser4/8 was shown to be required for promoting genome stability after replication stress (Ashley et al., 2014). In agreement with this, we observed moderately elevated genome instability in cells depleted of FBH1 following fork stalling, as evidenced by the increased presence of 53BP1 bodies in G1 phase. We hypothesize that the FBH1-mediated response is of prime importance when two approaching neighboring forks stall and collapse, leaving an unreplicated area in between. This is a very dangerous situation, because dormant origins are not available to rescue the unreplicated DNA. However, the FBH1 response promotes checkpoint signaling from such stalled forks that eventually can allow time for fork restart and DNA repair pathways to complete replication.

Our present findings may also help explain the strong ATM signaling in the context of the checkpoint tumorigenesis barrier in early lesions experiencing replication stress (Halazonetis et al., 2008). That ATM signaling has been attributed to eventual breakage of DNA at forks leading to DNA DSB formation, but we suggest that the novel FBH1-mediated checkpoint activation following replication fork stalling could in some circumstances contribute to such disease-associated ATM signaling. In this regard, it is noteworthy that mutations in *FBH1* have recently been demonstrated in melanoma cell lines, which exhibit increased survival in response to replication stress (Jeong et al., 2013a).

EXPERIMENTAL PROCEDURES

Cells, Chemicals, and siRNA

The human osteosarcoma cell line (U2OS) and human lung fibroblasts (TIG3) were grown in DMEM with 10% FBS in case of TIG3 supplemented by non-essential amino acids (GIBCO). U2OS cell lines carrying inducible expression vectors of GFP-hFBH1 and shRNA were described previously (Fugger et al., 2009). The following drugs were used in this study: hydroxyurea (Sigma), camptothecin (Sigma), aphidicolin (Sigma), nocodazole (Sigma), thymidine (Sigma), and ATM inhibitor (KU55933; Tocris Bioscience). For siRNA transfections, Lipofectamine RNAiMAX (Invitrogen) was used according to the manufacturer's instructions, with the modification that the transfection reagent was removed 4–6 hr after addition and fresh media added. For FBH1 transfection, a mix of siRNA nos. 1–3 was used, unless otherwise stated. The siRNA sequences used in this study are:

FBH1 no. 1 3′ UTR (5′GGGAUGUUCUUUUGAUAAAUU3′)
FBH1 no. 2 (5′GUGCCUAUUUGGUGUAAGA3′)
FBH1 no. 3 (5′AAACAAAACCUCGUCAUUA3′)
RAD51 (5′UUGAGACUGGAUCUAUCAC3′)
CtIP1 (5′GCUAAAACAGGAACGAAUC3′)
MUS81 (5′CAGCCCUGGUGGAUCGAUA3′)

Culture of MESCs

Plates for the MESC culture were coated using 0.1% type-A gelatin (Sigma) for 5 min before used. MESCs were maintained in 50% Buffalo rat liver (BRL)-conditioned medium/50% fresh DMEM supplemented with 10% fetal calf serum, 0.1% β-mercaptoethanol, 2.4 mM glutamine, 1,000 U/ml leukemia inhibitory factor (GIBCO), and non-essential amino acids. Cells were grown at 37°C in a humidified atmosphere containing 5% CO_2.

Flow Cytometry

To prepare cells for flow cytometry, U2OS cells were fixed in 70% ethanol. The cells were stained with the indicated antibodies for 1 hr followed by 1 hr incubation with Alexa-Fluor-conjugated secondary antibodies (Invitrogen; 1:1,000). DNA was stained with 0.1 mg/ml propidium iodide (PI) containing RNase (20 μg/ml) for 30 min at 37°C. For EdU labeling, cells were incubated with 10 μM EdU for 30 min before harvest. Click-it reaction was performed according to the manufacturer's description (Invitrogen). Flow cytometry was performed on a FACS Calibur (BD Biosciences) using CellQuest Pro software (Becton Dickinson).

Immunoblotting and Antibodies

For immunoblotting, cells were lysed on ice in cold EBC buffer (150 mM NaCl, 50 mM Tris [pH 7.4], 1 mM EDTA, and 0.5% NP-40/Igepal) containing protease inhibitors (1% aprotinin, 5 μg/ml leupeptin, and 1 mM PMSF), phosphatase inhibitors (50 mM NaF, β-glycerophosphate, and 0.5 μM Calyculin A), and 1 mM DTT. The lysates were sonicated using a digital sonifier (102C CE Converter; Branson). Proteins were separated by SDS-PAGE and transferred to a nitrocellulose membrane. Blocking and blotting with primary antibodies were performed in PBS-T supplemented with 5% skimmed milk powder. Proteins were visualized on films using secondary HRP-conjugated antibodies (1:10,000; Vector Laboratories) and ECL (GE Healthcare). Films were developed using an automated developer (Valsoe; Ferrania Technologies). All immunoblots shown are representative of at least three independent experiments. The following commercial rabbit antibodies were used in this study: phospho-CHK1-S317 (no. 2344; Cell Signaling Technology), phospho-CHK2-T68 (no. 2661; Cell Signal), phospho-p53-S15 (no. 9284; Cell Signal), phospho-KAP1-S824 (ab70369; Abcam), vinculin (V9131; Sigma), CtIP (BL1914; Bethyl Labs), phospho-RPA2-S4/8 (A300-245; Bethyl Labs), phospho-histone H3-S10 (06-570; Millipore), and RAD51 (H-92; SCBT). The following commercial mouse antibodies were used in this study: CHK1 (DCS-310; SCBT), CHK2 (DCS-270; SCBT), RPA (NA19L; Calbiochem), γH2AX (JBW301; Millipore), ATM (ATM 11G12; Abcam), phospho-ATM-S1981 (10H11.E12; Millipore), GFP (anti-GFP; Roche), and MUS81 (MTA30 2G10; Abcam). Rat antibody against RPA2 (4E4; Cell Signal) was used for detection of RPA2 in mouse cells. Rabbit antibodies raised against hFBH1 were described previously (Fugger et al., 2009; Jeong et al., 2013b).

Immunofluorescence

Cells were grown on coverslips and treated as indicated in the figure legends. The coverslips were fixed and stained as described previously (Fugger et al., 2009). Briefly, the coverslips were fixed in Lillies with or without prior pre-extraction in CSK buffer (0.5% Triton X-100 in 20 mM HEPES [pH 7.4], 50 mM NaCl, 3 mM MgCl, and 300 mM sucrose), permeabilized in 0.2% Triton X-100/PBS, and incubated with the indicated antibodies diluted in DMEM supplemented with 10% serum. Samples were then stained with secondary Alexa-Fluor-conjugated antibodies and mounted on glass slides using Vectashield mounting medium with DAPI (Vector Laboratories).

Single-Cell Image Analysis of 53BP1 Foci in G1 Phase

TIG3 cells were transfected with siRNA for 56 hr. Cells were treated with 2 mM HU for 18 hr followed by release into new medium for another 24 hr. Cells were fixed in 4% PFA for 15 min, washed by PBS, and permeabilized in PBS

supplemented with 5% Triton-X. The fixed cells were immunostained by first incubating in blocking solution (DMEM + 20% fetal serum) for 1 hr followed by incubation with 53BP1 primary antibody (Santa Cruz Biotechnology; rabbit, H-300; 1:300) and cyclin A (Lieca; mouse; 1:50) for 1 hr. Cells were washed three times with PBS, followed by incubation with secondary Alexa Fluor antibodies (Life Technologies; 1:1,000) dissolved in the blocking solution, followed by three washes in PBS. After the last wash, cells dishes were incubated in 1 μg/ml DAPI (Sigma) in dH2O for 5 min and air dried. Dried and stained cells were mounted using Vecta Shield (H-1000; Vector Labs) mounting medium. Images were automatically acquired using ScanR microscope system (Olympus) with a 20× water immersion objective (UApo/340W; 0.70 W) to obtain minimum 5,000 G1 cells per sample. In the analysis, G1 cells were selected as cells negative for cyclin A signal and at the same time spanning the G1 area according to the DAPI staining (see Figure S3D). 53BP1 foci were detected using the "spot detection" function of the ScanR Analysis software (Olympus). Experiments were done in three biologically independent replicates, and data were statistically processed.

PFGE

For DNA break analysis, 10^6 cells were melted into each agarose insert. The agarose inserts were incubated in proteinase K buffer (0.5 M EDTA, 1% *N*-laurylsarcosyl, and 1 mg/ml proteinase K) at 50°C for 48 hr and thereafter washed four times in TE buffer prior to loading onto a 1% agarose gel (chromosomal grade; Bio-Rad) and separated by CHEF DR III PFGE apparatus for 20 hr (Bio-Rad; 120° angle; 60–240 s switch time; 4 V/cm). The gel was subsequently stained with ethidium bromide and analyzed with Image Gauge software (FLA-3000; Fujifilm). All PFGE figures are representative of at least three independent experiments.

EM

In vivo psoralen crosslinking, isolation of total genomic DNA, and enrichment of the replication intermediates and their EM visualization were performed as described previously (Neelsen et al., 2014). In brief, cells were collected by trypsinization and genomic DNA was crosslinked by two rounds of incubation in 10 μM 4,5′,8-trimethylpsoralen and 2 min of irradiation with 366-nm UV light. Cells were lysed, and genomic DNA was isolated from the nuclei by proteinase K digestion and phenol-chloroform extraction. Purified DNA was digested with PvuII, and replication intermediates were enriched on a BND cellulose column. The DNA was spread on carbon-coated grids and visualized by platinum rotary shadowing. Images were acquired on a transmission electron microscope (G2 Spirit; FEI Tecnai) and analyzed with ImageJ (NIH). Analysis of replication intermediates using EM was performed in three independent biological experiments.

In Vitro Fork-Regression Assay

Fork-regression assays were performed as described previously (Ralf et al., 2006). The replication fork substrate (5 pM) was incubated with the indicated concentrations of either FBH1, BLM, or RecG in buffer H (50 mM Tris-HCl [pH 7.5], 50 mM NaCl, 2 mM $MgCl_2$, 2 mM ATP, 1 mM DTT, and 100 μg/ml BSA). Reactions were incubated for 30 min at 37°C and were then quenched with 5 mM AMP-PNP and 125 ng of M13 ssDNA. Reactions were then incubated with EcoRI for a further 30 min, and the reaction products were separated on a 10% polyacrylamide gel. Gels were dried and exposed to PhosphorImaging screens for analysis and quantification using a Typhoon FLA 7000 scanner (GE Healthcare). Fork-regression assays were performed at least three times, and representative figures are shown.

BrdU-Based Indirect Fork-Regression Assay

The BrdU assay was performed essentially as previously described (Couch et al., 2013). Briefly, U2OS cells were seeded on coverslips and transfected with siRNA for 48 hr. Cells were treated with 10 μM BrdU for 10 min and washed in fresh media before treatment or not with 2 mM HU for 4 hr. Cells were fixed with 4% formaldehyde and immunostained with anti-BrdU antibody (RPN20AB; GE Life Sciences) under native conditions. Images were acquired using AxioVert microscope. Image analysis and statistical analysis were performed using Volocity and Graphpad Prism 6 software, respectively. For analyzing ssDNA formation in GFP-FBH1-inducible cell lines, cells were treated as above, pre-extracted (PBS supplemented with 0.2% Triton X-100 for 2 min on ice), and co-stained for PCNA (Immuno Concepts no. 2037) Quantification was performed by automated multichannel fluorescence microscopy on an Olympus ScanR system (motorized IX81 microscope) with ScanR Image Acquisition Software and an UPLSAPO 10×/0.4 dry objective, fast-switching excitation and emission filter wheels for DAPI, Cy3 and Cy5 fluorescent dyes, an MT20 Illumination system, and a digital monochrome Hamamatsu C9100 electron-multiplying CCD camera. Image information of more than 2,000 cells per condition was acquired under non-saturating conditions; BrdU fluorescence intensity in PCNA-positive cells was quantified using the ScanR Image Analysis Software. Spotfire data visualization software (TIBCO) and Graphpad Prism 6 were used for statistical analysis.

SUPPLEMENTAL INFORMATION

Supplemental Information includes three figures and can be found with this article online at http://dx.doi.org/10.1016/j.celrep.2015.02.028.

AUTHOR CONTRIBUTIONS

K.F. and C.S.S. conceived the project; K.J.N., R.Z., and M.L. performed EM experiments and analyzed data; M.M. and J.B. performed genome integrity experiments (53BP1 foci formation) and analyzed the data; Q.Y., W.K.C., and I.D.H. performed in vitro fork-regression experiments; and K.F., A.N.K., and P.H. designed and performed all other experiments. M.M., K.J.N., and Q.Y. contributed equally. K.F. and C.S.S. drafted the manuscript; K.F., C.S.S., J.B., M.L., and I.D.H. wrote the manuscript; and all authors discussed the results and commented on the manuscript.

ACKNOWLEDGMENTS

This work was supported by The Novo Nordisk Foundation, The Danish Cancer Society, The Lundbeck Foundation, The Association for International Cancer Research, The European Research Council, The Nordea Foundation, The European Commission project DDResponse, Czech national program of sustainability LO1304, the Czech Ministry of Interior (VG20102014001), The Villum Kann Rasmussen Fund, The Danish National Research Foundation, and The Danish Medical Research Council. We thank the Center for Microscopy and Image Analysis of the University of Zurich for technical assistance with the EM experiments. K.J.N., R.Z., and M.L. were supported by Swiss National Science Foundation and Krebsliga Schweiz.

Received: August 26, 2014
Revised: December 12, 2014
Accepted: February 6, 2015
Published: March 12, 2015

REFERENCES

Ashley, A.K., Shrivastav, M., Nie, J., Amerin, C., Troksa, K., Glanzer, J.G., Liu, S., Opiyo, S.O., Dimitrova, D.D., Le, P., et al. (2014). DNA-PK phosphorylation of RPA32 Ser4/Ser8 regulates replication stress checkpoint activation, fork restart, homologous recombination and mitotic catastrophe. DNA Repair (Amst.) *21*, 131–139.

Atkinson, J., and McGlynn, P. (2009). Replication fork reversal and the maintenance of genome stability. Nucleic Acids Res. *37*, 3475–3492.

Branzei, D., and Foiani, M. (2010). Maintaining genome stability at the replication fork. Nat. Rev. Mol. Cell Biol. *11*, 208–219.

Bunting, S.F., Callén, E., Wong, N., Chen, H.T., Polato, F., Gunn, A., Bothmer, A., Feldhahn, N., Fernandez-Capetillo, O., Cao, L., et al. (2010). 53BP1 inhibits homologous recombination in Brca1-deficient cells by blocking resection of DNA breaks. Cell *141*, 243–254.

Ciccia, A., and Elledge, S.J. (2010). The DNA damage response: making it safe to play with knives. Mol. Cell *40*, 179–204.

Cimprich, K.A., and Cortez, D. (2008). ATR: an essential regulator of genome integrity. Nat. Rev. Mol. Cell Biol. *9*, 616–627.

Couch, F.B., Bansbach, C.E., Driscoll, R., Luzwick, J.W., Glick, G.G., Bétous, R., Carroll, C.M., Jung, S.Y., Qin, J., Cimprich, K.A., and Cortez, D. (2013). ATR phosphorylates SMARCAL1 to prevent replication fork collapse. Genes Dev. *27*, 1610–1623.

Fugger, K., Mistrik, M., Danielsen, J.R., Dinant, C., Falck, J., Bartek, J., Lukas, J., and Mailand, N. (2009). Human Fbh1 helicase contributes to genome maintenance via pro- and anti-recombinase activities. J. Cell Biol. *186*, 655–663.

Fugger, K., Chu, W.K., Haahr, P., Kousholt, A.N., Beck, H., Payne, M.J., Hanada, K., Hickson, I.D., and Sørensen, C.S. (2013). FBH1 co-operates with MUS81 in inducing DNA double-strand breaks and cell death following replication stress. Nat. Commun. *4*, 1423.

Halazonetis, T.D., Gorgoulis, V.G., and Bartek, J. (2008). An oncogene-induced DNA damage model for cancer development. Science *319*, 1352–1355.

Hanada, K., Budzowska, M., Davies, S.L., van Drunen, E., Onizawa, H., Beverloo, H.B., Maas, A., Essers, J., Hickson, I.D., and Kanaar, R. (2007). The structure-specific endonuclease Mus81 contributes to replication restart by generating double-strand DNA breaks. Nat. Struct. Mol. Biol. *14*, 1096–1104.

Harrigan, J.A., Belotserkovskaya, R., Coates, J., Dimitrova, D.S., Polo, S.E., Bradshaw, C.R., Fraser, P., and Jackson, S.P. (2011). Replication stress induces 53BP1-containing OPT domains in G1 cells. J. Cell Biol. *193*, 97–108.

Hickson, I., Zhao, Y., Richardson, C.J., Green, S.J., Martin, N.M., Orr, A.I., Reaper, P.M., Jackson, S.P., Curtin, N.J., and Smith, G.C. (2004). Identification and characterization of a novel and specific inhibitor of the ataxia-telangiectasia mutated kinase ATM. Cancer Res. *64*, 9152–9159.

Jackson, S.P., and Bartek, J. (2009). The DNA-damage response in human biology and disease. Nature *461*, 1071–1078.

Jeong, Y.T., Cermak, L., Guijarro, M.V., Hernando, E., and Pagano, M. (2013a). FBH1 protects melanocytes from transformation and is deregulated in melanomas. Cell Cycle *12*, 1128–1132.

Jeong, Y.T., Rossi, M., Cermak, L., Saraf, A., Florens, L., Washburn, M.P., Sung, P., Schildkraut, C.L., and Pagano, M. (2013b). FBH1 promotes DNA double-strand breakage and apoptosis in response to DNA replication stress. J. Cell Biol. *200*, 141–149.

Kim, J., Kim, J.H., Lee, S.H., Kim, D.H., Kang, H.Y., Bae, S.H., Pan, Z.Q., and Seo, Y.S. (2002). The novel human DNA helicase hFBH1 is an F-box protein. J. Biol. Chem. *277*, 24530–24537.

Laulier, C., Cheng, A., Huang, N., and Stark, J.M. (2010). Mammalian Fbh1 is important to restore normal mitotic progression following decatenation stress. DNA Repair (Amst.) *9*, 708–717.

Li, S., Ting, N.S., Zheng, L., Chen, P.L., Ziv, Y., Shiloh, Y., Lee, E.Y., and Lee, W.H. (2000). Functional link of BRCA1 and ataxia telangiectasia gene product in DNA damage response. Nature *406*, 210–215.

Liaw, H., Lee, D., and Myung, K. (2011). DNA-PK-dependent RPA2 hyperphosphorylation facilitates DNA repair and suppresses sister chromatid exchange. PLoS ONE *6*, e21424.

Lorenz, A., Osman, F., Folkyte, V., Sofueva, S., and Whitby, M.C. (2009). Fbh1 limits Rad51-dependent recombination at blocked replication forks. Mol. Cell. Biol. *29*, 4742–4756.

Lukas, C., Savic, V., Bekker-Jensen, S., Doil, C., Neumann, B., Pedersen, R.S., Grøfte, M., Chan, K.L., Hickson, I.D., Bartek, J., and Lukas, J. (2011). 53BP1 nuclear bodies form around DNA lesions generated by mitotic transmission of chromosomes under replication stress. Nat. Cell Biol. *13*, 243–253.

Masuda-Ozawa, T., Hoang, T., Seo, Y.S., Chen, L.F., and Spies, M. (2013). Single-molecule sorting reveals how ubiquitylation affects substrate recognition and activities of FBH1 helicase. Nucleic Acids Res. *41*, 3576–3587.

Neelsen, K.J., Zanini, I.M., Herrador, R., and Lopes, M. (2013a). Oncogenes induce genotoxic stress by mitotic processing of unusual replication intermediates. J. Cell Biol. *200*, 699–708.

Neelsen, K.J., Zanini, I.M., Mijic, S., Herrador, R., Zellweger, R., Ray Chaudhuri, A., Creavin, K.D., Blow, J.J., and Lopes, M. (2013b). Deregulated origin licensing leads to chromosomal breaks by rereplication of a gapped DNA template. Genes Dev. *27*, 2537–2542.

Neelsen, K.J., Chaudhuri, A.R., Follonier, C., Herrador, R., and Lopes, M. (2014). Visualization and interpretation of eukaryotic DNA replication intermediates in vivo by electron microscopy. Methods Mol. Biol. *1094*, 177–208.

Petermann, E., Orta, M.L., Issaeva, N., Schultz, N., and Helleday, T. (2010). Hydroxyurea-stalled replication forks become progressively inactivated and require two different RAD51-mediated pathways for restart and repair. Mol. Cell *37*, 492–502.

Ralf, C., Hickson, I.D., and Wu, L. (2006). The Bloom's syndrome helicase can promote the regression of a model replication fork. J. Biol. Chem. *281*, 22839–22846.

Ray Chaudhuri, A., Hashimoto, Y., Herrador, R., Neelsen, K.J., Fachinetti, D., Bermejo, R., Cocito, A., Costanzo, V., and Lopes, M. (2012). Topoisomerase I poisoning results in PARP-mediated replication fork reversal. Nat. Struct. Mol. Biol. *19*, 417–423.

Ryan, A.J., Squires, S., Strutt, H.L., and Johnson, R.T. (1991). Camptothecin cytotoxicity in mammalian cells is associated with the induction of persistent double strand breaks in replicating DNA. Nucleic Acids Res. *19*, 3295–3300.

Sartori, A.A., Lukas, C., Coates, J., Mistrik, M., Fu, S., Bartek, J., Baer, R., Lukas, J., and Jackson, S.P. (2007). Human CtIP promotes DNA end resection. Nature *450*, 509–514.

Simandlova, J., Zagelbaum, J., Payne, M.J., Chu, W.K., Shevelev, I., Hanada, K., Chatterjee, S., Reid, D.A., Liu, Y., Janscak, P., et al. (2013). FBH1 helicase disrupts RAD51 filaments in vitro and modulates homologous recombination in mammalian cells. J. Biol. Chem. *288*, 34168–34180.

Thompson, L.H. (2012). Recognition, signaling, and repair of DNA double-strand breaks produced by ionizing radiation in mammalian cells: the molecular choreography. Mutat. Res. *751*, 158–246.